Article

Theoretical Studies of Stereoselectivities of Intramolecular Aldol Cyclizations Catalyzed by Amino Acids

Fernando R. Clemente, and K. N. Houk

J. Am. Chem. Soc., **2005**, 127 (32), 11294-11302• DOI: 10.1021/ja0507620 • Publication Date (Web): 23 July 2005

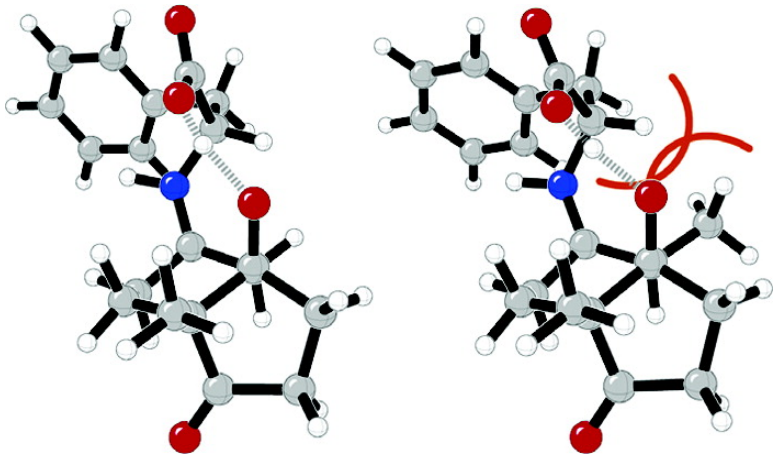

J|A|C|S
ARTICLES
Published on Web 07/23/2005

Theoretical Studies of Stereoselectivities of Intramolecular Aldol Cyclizations Catalyzed by Amino Acids

Fernando R. Clemente and K. N. Houk*

Contribution from the Department of Chemistry and Biochemistry, University of California, Los Angeles, California 90095-1569

Received February 4, 2005; E-mail: houk@chem.ucla.edu

Abstract: The effects of different amino acid catalysts and substrate substituents on the stereoselectivity of the title reactions have been studied with the aid of density functional theory methods. Experimental data available in the literature have been compiled. B3LYP/6-31G(d) calculations match the general experimental trends and provide useful insights into the origins of the variations in stereoselectivities. Acyclic primary amino acids allow a greater conformational flexibility in the aldol transition states compared with proline. This makes them poorer enantioselective catalysts with triketone substrates with a methyl ketone side chain. The steric repulsion upon substitution at the terminal methyl group increases the energy difference between anti- and syn-chairs with primary amino acid catalysts and, consequently, the stereoselectivities. Proline, in contrast, is a poor catalyst for the latter reactions because the substituent's steric bulkiness raises the activation energy of the favored C−C bond-forming pathway.

Background

The proline-catalyzed intramolecular aldol cyclization of triketones **1** (Scheme 1) is recognized today as one of the first contributions to enantioselective organocatalysis. In the early 1970s, two groups, Hajos and Parrish at Hoffmann La Roche, and Eder, Sauer, and Wiechert at Schering AG, published a series of papers and patents involving these transformations.[1] This discovery made possible the stereoselective synthesis of enediones **3**, like the so-called Wieland−Miescher ketone (n = 2, R^1 = H, R^2 = Me), which have proven to be particularly useful building blocks for steroid, terpenoid, and taxol total syntheses.[2]

Hajos and Parrish found that the (*S*)-proline-catalyzed (3−100% eq) cyclizations of **1** into (*S*,*S*)-**2** at room temperature proceeded, in polar aprotic solvents (DMF, CH_3CN), with excellent chemical yields (95−100%) and ee's (90−96%). When the reactions were carried out in alcoholic solution, the enantioselectivity decreased drastically (27−83% ee), thus suggesting a key role of hydrogen-bonding in the stereocontrol.

On the other hand, Eder, Sauer, and Wiechert conducted the reactions in the presence of an acid as cocatalyst ($HClO_4$, HCl)

Scheme 1

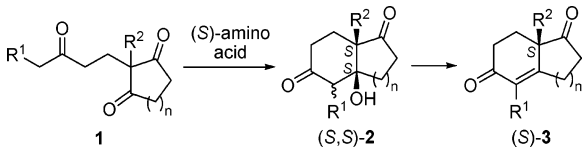

at higher temperatures (80−100 °C) than in the Hajos−Parrish procedures. Under these reaction conditions, the aldol adduct **2** is not isolated, and the bicyclic enediones (*S*)-**3** are obtained in shorter reaction times with lower, although still good, chemical yields (69−87%) and ee's (69−84%).

A variety of amino acids have been used to catalyze this enantioselective transformation (Scheme 1), and in all cases, (*S*)-α-amino acids induced the preferential formation of (*S*)-enediones while opposite results were obtained with (*R*)-α-amino acids (Table 1). The highest ee's in the cyclization of methyl ketones (**1**, R^1 = H) were obtained using the secondary cyclic amino acids proline[1,3,4] (∼95% with n = 1 and ∼75% with n = 2) or *trans*-4-hydroxyproline and its *O*-derivatives (∼75%).[1,5] In contrast, primary amino acids like phenylalanine[1a,b,3a] proved to be poor catalysts for this transformation and gave much lower enantioselectivity (<25%).

When R^1 of the starting triketone is not a hydrogen atom (**1**, R^1 = alkyl, aralkyl, oxoalkyl, arylthio), the pattern of stereoselectivities is quite different. In these cases, primary amino

(1) (a) Hajos, Z. G.; Parrish, D. R. German Patent DE 2102623, Jul 29, 1971. (b) Hajos, Z. G.; Parrish, D. R. *J. Org. Chem.* **1974**, *39*, 1615−1621. (c) Eder, U.; Sauer, G.; Wiechert, R. German Patent DE 2014757, Oct 7, 1971. (d) Eder, U.; Sauer, G.; Wiechert, R. *Angew. Chem., Int. Ed. Engl.* **1971**, *10*, 496−497. (e) Ruppert, J.; Eder, U.; Wiechert, R. *Chem. Ber.* **1973**, *106*, 3636−3644.

(2) (a) Danishefsky, S.; Cain, P. *J. Am. Chem. Soc.* **1976**, *98*, 4975−4983. (b) Cohen, N. *Acc. Chem. Res.* **1976**, *9*, 412−417. (c) Smith, A. B., III; Kingery-Wood, J.; Leenay, T. L.; Nolen, E. G.; Sunazuka, T. *J. Am. Chem. Soc.* **1992**, *114*, 1438−1449. (d) Nagamitsu, T.; Sunazuka, T.; Obata, R.; Tomoda, H.; Tanaka, H.; Harigaya, Y.; Omura, S.; Smith, A. B., III. *J. Org. Chem.* **1995**, *60*, 8126−8127. (e) Pemp, A.; Seifert, K. *Tetrahedron Lett.* **1997**, *38*, 2081−2084. (f) Danishefsky, S. J.; Masters, J. J.; Young, W. B.; Link, J. T.; Snyder, L. B.; Magee, T. V.; Jung, D. K.; Isaacs, R. C. A.; Bornmann, W. G.; Alaimo, C. A.; Coburn, C. A.; DiGrandi, M. J. *J. Am. Chem. Soc.* **1996**, *118*, 2843−2859.

(3) (a) Buchschacher, P.; Cassal, J.-M.; Fürst, A.; Meier, W. *Helv. Chim. Acta* **1977**, *60*, 2747−2755. (b) Takano, S.; Kasahara, C.; Ogasawara, K. *J. Chem. Soc., Chem. Commun.* **1981**, 635−637. (c) Tamai, Y.; Mizutani, Y.; Hagiwara, H.; Uda, H.; Harada, N. *J. Chem. Res. (M)* **1985**, 1746−1787. (d) Rajagopal, D.; Narayanan, R.; Swaminathan, S. *Tetrahedron Lett.* **2001**, *42*, 4887−4890.

(4) Hoang, L.; Bahmanyar, S.; Houk, K. N.; List, B. *J. Am. Chem. Soc.* **2003**, *125*, 16−17.

(5) Bui, T.; Barbas, C. F., III. *Tetrahedron Lett.* **2000**, *41*, 6951−6954.

10.1021/ja0507620 CCC: $30.25

Table 1. Yields and Enantioselectivities of Intramolecular Aldol Reactions of Triketones **1** Catalyzed by Proline and Acyclic Amino Acids

	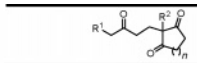													
	n	R^1	R^2	Yield (%)	ee (%)	Proc.[a]	time (h)	Ref.	Yield (%)	ee (%)	Proc.[a]	time (h)	aa	Ref.
a	1	—H	—Me	69-76	72-83	(i)	3.5-26	1c	37	19	(ii)	168	Phe	1a,b
				87	84	(i)	22	1d	85	25	(ii)	384	Phe	3a
				95-100	90-96	(ii)	20-144	1a,b	91	20	(i)	55	Phe	3a
				63-66	60-68	(vi)	88-90	6	0	0	(ii)	168	*t*-Leu	7a
				n/a[b]	88-90	(ii)	6.5-24	4	95	2	(i)	68	*t*-Leu	7a
				87-97	92-94	(ii)	42-46	3a						
				90	82	(i)	23	3a						
				70	77	(ii)	n/a[b]	3d						
				54	49	(vi)	n/a[b]	3d						
				12[c]	73[c]	(ii)	624	1a,b						
				8[d]	0[d]	(ii)	432	1b						
				58[e]	27[e]	(ii)	24	8						
				0[f]	0[f]	(ii)	5000	8						
				51[g]	64[g]	(ii)	144	1a,b						
b	1	—H	—Et	76	80	(i)	7	1d						
				98	95	(ii)	20	1a,b						
c	1	—Me	—Me	39	93	(ii)	120	9	65	71	(i)	65	Ala	1c
				27-70	72-100	(v)	35-159	9	76	66	(i)	45	Phe	1c
									69	68	(i)	70	Ala	1d
									80	74	(i)	72	Val	10
d	1		—Me	22-55	0-20	(i)	45-120	11a	21-85	45-76	(i)	12-72	Phe	11a
									77	17	(iv)	26	Phe	11a
									40	68	(i)	65	Trp	11a
									64	24	(i)	37	Tyr	11a
									22	0	(i)	74	Ala	11a
e	1		—Me	50	0	(i)	n/a[b]	7b	55	64	(iv)	4	Phe	1d
									50	65	(iv)	4	Trp	7b
									73-79	88	(i)	72-74	*t*-Leu	7a
									70	86	(iv)	4	*t*-Leu	7a
f	1		—Et						85	95	(i)	70	Phe	7b
									50	80	(iv)	4	Phe	7b
									59	77	(iv)	4	Trp	7b
									63-73	44-45	(i)	68	*t*-Leu	7a
g	1	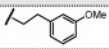	—Me	76	45	(ii)	38	1a	67	85	(i)	48	Phe	1c
									60	92	(i)	43	Phe	1d
h	1	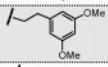	—Me						78	66	(i)	240	Phe	12
i	1	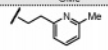	—Me	67	26	(i)	n/a[b]	2a	80-82	80-86	(i)	40-n/a[b]	Phe	2a
									82	84	(i)	n/a[b]	Tyr-OMe	2a
									70	78 (*R*)	(i)	n/a[b]	(*R*)-Trp	2a
									77	35	(i)	n/a[b]	Ser	2a
									72	21	(i)	n/a[b]	Val	2a
j	1		—Me	44-60	10-57	(ii)	18	11e	69-71	89	(iii)	96	Phe	11e
				50	54	(iii)	96	11e						
k	2	—H	—Me	80	69	(i)	18	1e						
				83	71	(i)	25	1d						
				91	73	(ii)	192	1a						
				59	63	(vi)	67	6						
				71	70	(ii)	120	13						
				n/a[b]	76	(ii)	24	4						
				49	76	(ii)	n/a[b]	5						
				n/a[b,c]	60-75[c]	(ii)	n/a[b]	5						
				n/a[b,g]	<10[g]	(ii)	n/a[b]	5						
				68	63	(ii)	n/a[b]	3d						
				45	44	(vi)	n/a[b]	3d						
l	2	—H	—OMEM[h]	57-70	72-75	(ii)	21-25	3c	70	4	(ii)	n/a[b]	Phe	3c
m	2	—Me	—Me	43-60	17-28	(ii)	480-816	14	70-83	80-91	(iii)	120	Phe	11c
									86	85	(iii)	n/a[b]	Phe	11b
n	2	—Me	—OMe						86	86 (*R*)	(i)	165	(*R*)-Phe	3c
									39	86 (*R*)	(ii)	192	(*R*)-Phe	3c
o	2	—Me	—OAc						56-77	88 (*R*)	(i)	46-184	(*R*)-Phe	3c
									77-90	90-96	(iii)	144-210	Phe	3c
									80	87 (*R*)	(i)	181	(*R*)-Trp	3c
									87	89	(iii)	120	Trp	3c
p	2	—Me	—OMOM[i]						88	85	(iii)	140	Phe	3c
									86	89	(iii)	120	Trp	3c
q	2		—Me						77	95	(iii)	576	Phe	11d
r	2		—Me						50	n/a[b]	(iv)	n/a[b]	Phe	7b

[a]Typical procedures: (i) Wiechert: 1N HCl (aq) or $HClO_4$ (aq) cocatalyst (10% vol), refluxing CH_3CN.
(ii) Hajos (neutral): room temperature (15-35 °C) in a polar aprotic solvent (DMF, DMSO, CH_3CN).
(iii) Hagiwara: D-(+)-10-camphorsulfonic acid cocatalyst, DMF, temperature control from rt to 70 °C.
(iv) Refluxing acetic acid.
(v) Piperidine cocatalyst (base), DMF, 60 °C.
(vi) Neat, room temperature.

[b]Not available. [c]  . [d]  (bridged ketol in 20% yield). [e]  . [f]  (starting material). [g]  . [h] —OMEM = 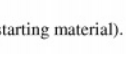 . [i] —OMOM =  .

acids are remarkably efficient catalysts in the asymmetric aldol cyclizations of these substrates (Table 1). Phenylalanine, tryptophan, alanine, valine, *tert*-leucine, or tyrosine *O*-methyl ether can catalyze the formation of enediones **3** ($R^1 \neq H$) in 70−96% optical yields with the aid of an acid cocatalyst (Table 1). All of these catalyst systems assisted the cyclization process more efficiently than proline. When this secondary amino acid was used under neutral conditions,[9] the products were obtained with good enantioselectivity (93% ee) but low chemical yields after long reaction times; when it was used in conjunction with an acid,[2a,11a] the reaction times were significantly shortened, but the ee's dropped to less than 30%. The latter results are easily explained, since acid conditions are known to catalyze a non-enantioselective pathway, thus yielding the products in lower ee's than in a neutral medium.[3a] In most cases, the reported ee's are subject to significant errors since they are based on polarimetric measurements and, for some of them, the optical rotation of the pure enantiomer is unknown. Cyclizations catalyzed by primary amino acids require a Brönsted acid cocatalyst which, in the case of HCl or $HClO_4$, is an aqueous solution (∼10% of the reaction mixture volume). For intramolecular aldol reactions catalyzed by proline, Barbas et al. reported a drop in enantioselectivity from ∼80% ee to ∼30% ee for anhydrous conditions versus 10 vol % water.[15] The presence of a strong Brönsted acid, significant amounts of water, and elevated temperatures (∼80 °C) are conditions needed to promote the reactions but they obviously promote non-stereoselective pathways that may become competitive and lower the enantioselectivities from the ones expected from a theoretical viewpoint. This seriously limits our ability to make quantitative predictions.

Hajos and Parrish initially proposed two possible mechanisms for these reactions. One of them involves the attack of proline on one of the cyclic carbonyl groups to form a carbinolamine intermediate; the subsequent C−C bond-forming step consists of the displacement of the proline moiety by nucleophilic attack of the side-chain enol (**A**, Scheme 2).[16] The other mechanism involves the attack of proline on the acyclic carbonyl group to form an enaminium intermediate that acts as the nucleophile in the subsequent C−C bond formation with concomitant N−H···O hydrogen transfer (**B**, Scheme 2).

Experimental evidence presented by Spencer[17] and Wakselman[18] suggests that a mechanism involving an enamine

Scheme 2. Mechanisms Proposed for the Proline-Catalyzed Intramolecular Aldol Reactions

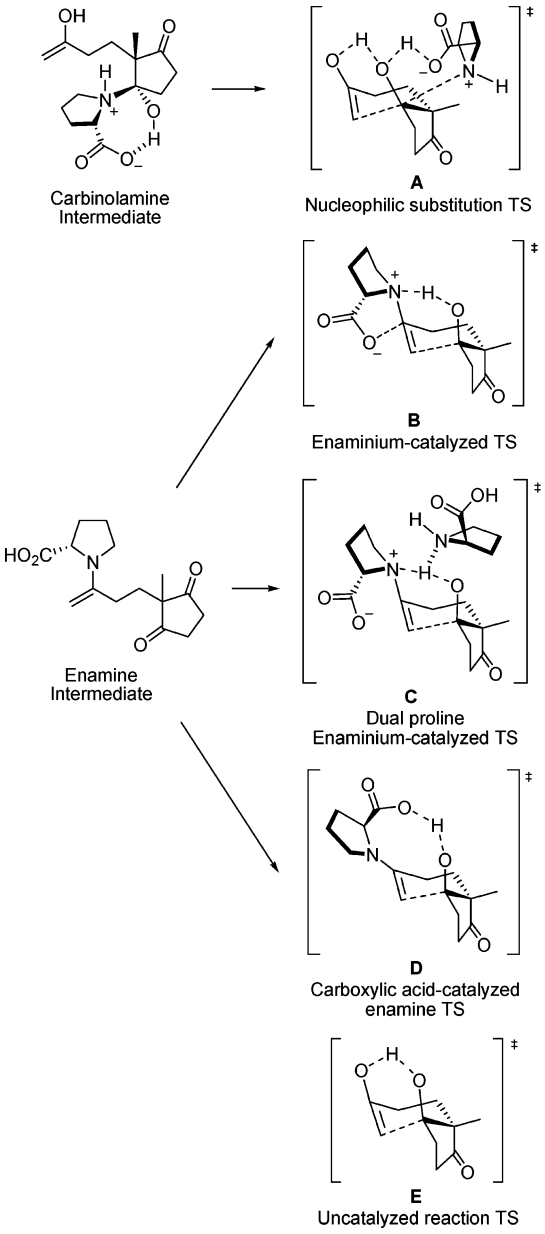

intermediate appears more feasible. In the 1980s, Agami et al.[19] proposed a modification of the original enaminium-catalyzed mechanism presented by Hajos and Parrish. The new mechanism (**C**, Scheme 2) invoked the presence of a second proline molecule assisting in the N−H···O hydrogen transfer, thus enabling conjugation of the nitrogen lone pair with the enamine system. This model was supported by polarimetric studies that indicated a small nonlinear kinetic effect, suggesting the involvement of several prolines in the stereoselectivity-determining step (**C**, Scheme 2).[20]

Mechanism **D** (Scheme 2) involves attack of an enamine intermediate accompanied by proton transfer from the proline carboxylic acid moiety to the developing alkoxide. This transi-

(6) Rajagopal, D.; Rajagopalan, K.; Swaminathan, S. *Tetrahedron: Asymmetry* **1996**, *7*, 2189−2190.
(7) (a) Wang, K. C.; Kan, W.-M.; Gau, C.-S. *J. Taiwan Pharm. Assoc.* **1986**, *38*, 6−9. (b) Wang, K. C.; Huang, J.-D. *J. Taiwan Pharm. Assoc.* **1978**, *30*, 160−169.
(8) Martens, J.; Lüben, S. *Arch. Pharm. (Weinheim)* **1991**, *324*, 59−60.
(9) Medarde, M.; Caballero, E.; Melero, C. P.; Tomé, F.; San Feliciano, A. *Tetrahedron: Asymmetry* **1997**, *8*, 2075−2077.
(10) Banerjee, D. K.; Kasturi, T. R.; Sarkar, A. *Proc. Indian Acad. Sci. (Chem. Sci.)* **1983**, *92*, 181−187.
(11) (a) Shimizu, I.; Naito, Y.; Tsuji, J. *Tetrahedron Lett.* **1980**, *21*, 487−490. (b) Takahashi, S.; Oritani, T.; Yamashita, K. *Agric. Biol. Chem.* **1987**, *51*, 2291−2293. (c) Hagiwara, H.; Uda, H. *J. Org. Chem.* **1988**, *53*, 2308−2311. (d) Corey, E. J.; Virgil, S. C. *J. Am. Chem. Soc.* **1990**, *112*, 6429−6431. (e) Przezdziecka, A.; Stepanenko, W.; Wicha, J. *Tetrahedron: Asymmetry* **1999**, *10*, 1589−1598.
(12) Mander, L. N.; Turner, J. V. *Tetrahedron Lett.* **1981**, *22*, 3683−3686.
(13) Gutzwiller, J.; Buchschacher, P.; Fürst, A. *Synthesis* **1977**, 167−168.
(14) Coisne, J.-M.; Pecher, J. *Bull. Soc. Chim. Belg.* **1981**, *90*, 481−484.
(15) Sakthivel, K.; Notz, W.; Bui, T.; Barbas, C. F., III. *J. Am. Chem. Soc.* **2001**, *123*, 5260−5267.
(16) (a) Jung, M. E. *Tetrahedron* **1976**, *32*, 3−31. (b) Corrected configuration of the carbinolamine intermediate as suggested in ref 16a.
(17) Spencer, T. A.; Neel, H. S.; Flechtner, T. W.; Zayle, R. A. *Tetrahedron Lett.* **1965**, *43*, 3889−3897.
(18) Molines, H.; Wakselman, C. *Tetrahedron* **1976**, *32*, 2099−2103.
(19) (a) Agami, C.; Meynier, F.; Puchot, C.; Guilhem, J.; Pascard, C. *Tetrahedron* **1984**, *40*, 1031−1038. (b) Agami, C. *Bull. Soc. Chim. Fr.* **1988**, *3*, 499−507.
(20) (a) Agami, C.; Levisalles, J.; Puchot, C. *J. Chem. Soc., Chem. Commun.* **1985**, 441−442. (b) Agami, C.; Puchot, C. *J. Mol. Catal.* **1986**, *38*, 341−343.

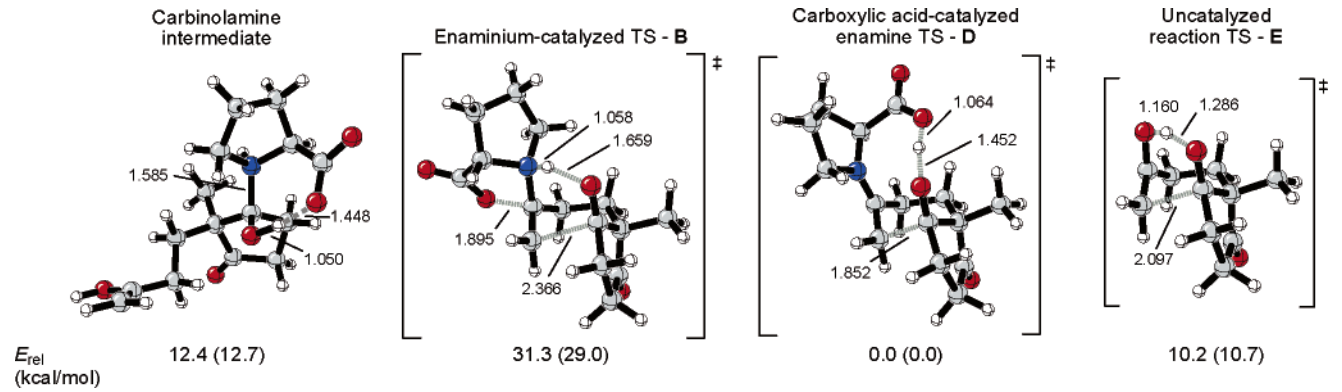

Figure 1. Energy comparison of three proposed proline-catalyzed aldolization mechanisms at the B3LYP/6-31+G(d,p)//B3LYP/6-31G(d) level. Values in parentheses include solvation energies in DMSO using the PCM/UAKS model.[25]

tion state (TS) model was introduced by Jung[16a] in a 1976 review and was favored by Eschenmoser in his extensive studies of enamine reactions.[21] This mechanism was almost abandoned in favor of Agami's model until the List and Barbas group proposed a transition state similar to **D** (although with participation of the proline nitrogen in the hydrogen transfer as in **B**) for the intermolecular aldol reactions catalyzed by proline.[22]

Recently, List et al.[23] have studied these aldol cyclizations using carefully dried substrate (triketone **1**), catalyst (proline), and solvent (DMSO), and then adding 3 vol % of ^{18}O-labeled water. Under these conditions, the aldol products were obtained showing an efficient (>90%) ^{18}O-incorporation, which questions the strongest support for the mechanism involving the nucleophilic substitution TS in the C−C bond-forming step (**A**).[1b] In collaboration with our group,[4] they observed a linear relationship between the ee's of catalyst and aldol product in these proline-catalyzed intramolecular cyclizations upon reinvestigation with modern chiral HPLC methods. The same has also been reported in the intermolecular case.[15] B3LYP/6-31G(d) computational studies[4] predict almost no enantioselectivity if an amine molecule assists the hydrogen transfer (a molecule of dimethylamine was used as a model for the second proline molecule proposed by Agami et al.). Thus, the experimental and theoretical studies presented therein support a one-proline mechanism.

Our comparative study of pathways **A**, **B**, **D**, and **E** (Scheme 2) at the key C−C bond-forming step[24] complements the recent experimental evidence[4,23] in establishing the long-debated mechanism of these reactions. The results with B3LYP/6-31+G(d,p)//B3LYP/6-31G(d) indicate that the carboxylic-acid-catalyzed model (**D**, Scheme 2) is lowest in energy and, therefore, the mechanism of the proline-catalyzed aldol cyclization that we favor (Figure 1). This pathway is ∼10 kcal/mol below the uncatalyzed process. The enaminium TS (**B**, Scheme 2) is clearly disfavored over the former (31 kcal/mol higher in energy), which confirms Agami's suggestions about the disadvantage of a protonated enamine moiety. All the attempts to locate the transition structure for the C−C bond-forming process through a nucleophilic substitution mechanism (**A**, Scheme 2) were unsuccessful. Instead, starting from reasonable TS geometry, optimization evolved in most of the cases through the departure of the proline molecule before the transition state and ended in a structure analogous to the product of the uncatalyzed process. In addition, the starting structure for that step, i.e., the carbinolamine intermediate, is ∼12 kcal/mol higher in energy than the carboxylic-acid-catalyzed TS. Therefore, the transition structure leading to the aldol product via **A** must be even higher in energy. This illustrates the difficulty of nucleophilic attack of an enol on a tertiary carbon as well as the lower nucleophilicity of enols with respect to enamines.

Computational Methods

All the calculations were carried out with Gaussian 98.[26] The geometries of all the stationary points were fully optimized at the B3LYP/6-31G(d)[27] level, and their nature (minimum or transition state) was determined by frequency analysis. In selected cases and for testing the effect of diffuse functions, we have performed full optimizations at the B3LYP/6-31+G(d,p) level and/or computed the energies at the B3LYP/6-31+G(d,p)//B3LYP/6-31G(d) level. A harmonic approximation was implemented for the calculation of the zero-point energy corrections, which are included in all of the reported energies.

Stereoselectivity in the Cyclizations of Methyl Ketones

Proline. In this decade, our group has performed a series of computational studies dealing with the different aspects of amine- and proline-catalyzed aldol, Mannich, and other related reactions.[4,24,28] B3LYP/6-31G(d) computational studies satisfactorily reproduce the experimental observations about the enantioselectivity of proline-catalyzed intramolecular aldol reactions (Figure 2).[28c] Figure 2 shows the transition structures for the cyclization of the proline enamines following the carboxylic-acid-catalyzed model (**D**). The (*S*,*S*)-enantiomer, the major one, is favored by more than 3 kcal/mol. The energy difference is somewhat overestimated over the experimental value, but it is consistent with the excellent ee (97% in CH_3CN) observed for this transformation.[1]

(21) Brown, K. L.; Damm, L.; Dunitz, J. D.; Eschenmoser, A.; Hobi, R.; Kratky, C. *Helv. Chim. Acta* **1978**, *61*, 3108−3135.
(22) List, B.; Lerner, R. A.; Barbas, C. F., III. *J. Am. Chem. Soc.* **2000**, *122*, 2395−2396.
(23) List, B.; Hoang, L.; Martin, H. J. *Proc. Natl. Acad. Sci. U.S.A.* **2004**, *101*, 5839−5842.
(24) Clemente, F. R.; Houk, K. N. *Angew. Chem., Int. Ed.* **2004**, *43*, 5766−5768.
(25) (a) Takano, Y.; Houk, K. N. *J. Chem. Theory Comput.* **2005**, *1*, 70−77. (b) Mennucci, B.; Cammi, R.; Tomasi, J. *J. Chem. Phys.* **1999**, *110*, 6858−6870. (c) Cossi, M.; Scalmani, G.; Rega, N.; Barone, V. *J. Chem. Phys.* **2002**, *117*, 43−54.
(26) Frisch, M. J.; et al. *Gaussian 98*, Revision A.9; Gaussian, Inc.: Pittsburgh, PA, 1998.
(27) (a) Becke, A. D. *J. Chem. Phys.* **1993**, *98*, 5648−5652. (b) Lee, C.; Yang, W.; Parr, R. G. *Phys. Rev. B* **1988**, *37*, 785−789.
(28) (a) Allemann, C.; Gordillo, R.; Clemente, F. R.; Cheong, P. H.; Houk, K. N. *Acc. Chem. Res.* **2004**, *37*, 558−569. (b) Bahmanyar, S.; Houk, K. N. *J. Am. Chem. Soc.* **2001**, *123*, 11273−11283. (c) Bahmanyar, S.; Houk, K. N. *J. Am. Chem. Soc.* **2001**, *123*, 12911−12912. (d) Bahmanyar, S.; Houk, K. N.; Martin, H. J.; List, B. *J. Am. Chem. Soc.* **2003**, *125*, 2475−2479. (e) Bahmanyar, S.; Houk, K. N. *Org. Lett.* **2003**, *5*, 1249−1251.

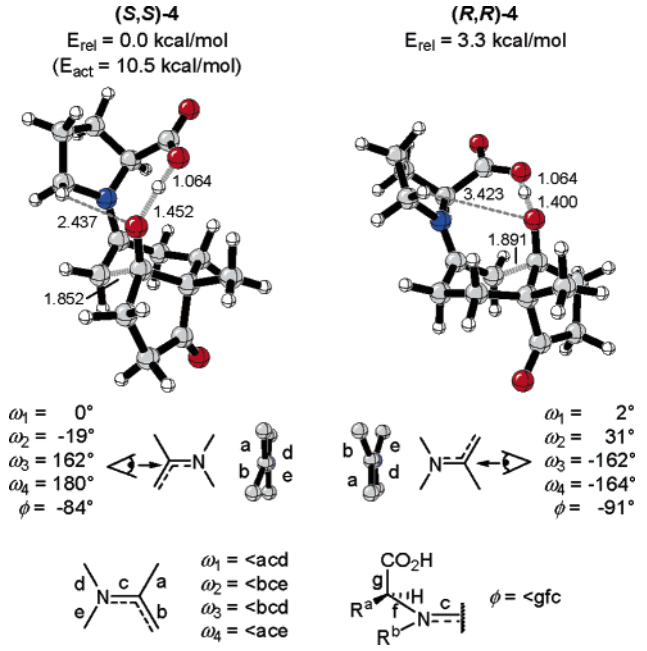

Figure 2. Transition states for proline-catalyzed cyclizations.

In (*S*,*S*)-**4**, the carboxylic acid group and the enamine double bond present an anti relationship with respect to the C−N axis, while in (*R*,*R*)-**4** this relationship is syn. In a syn disposition, the two oxygen atoms involved in the hydrogen transfer are too close to each other so, to achieve an optimal O−H···O arrangement, the enamine system is forced to be out of planarity ($\omega_{2(syn)} = 31°$ vs $\omega_{2(anti)} = -19°$, see Figure 2 for Newman projections).[29] In addition, in anti arrangements, a $^{\delta+}$NCH···O$^{\delta-}$ stabilizing electrostatic interaction also contributes to the lower energy of such transition structures ($d_{CH-O(anti)} = 2.44$ Å vs $d_{CH-O(syn)} = 3.42$ Å).[30]

The energy barrier for the cyclization of the proline enamine is much lower than that of the alkylamine enamines. Secondary amine enamines that are not able to transfer a proton to the developing alkoxide have the highest activation barriers, 33 kcal/mol.[28b] Cyclization of primary amine enamines involves hydrogen transfer to the developing alkoxide from the amine, and the activation barriers decrease to 22 kcal/mol. However, to achieve this N−H···O hydrogen transfer, there is a significant loss in conjugation between the nitrogen lone pair and the C=C double bond.[28b] The activation barrier for cyclization of proline enamine is only 10.5 kcal/mol (Figure 2), which involves activation of the carbonyl by hydrogen transfer to the developing alkoxide and a nearly planar enamine system.

This computational study also shows why the proline-catalyzed cyclizations of the acyclic diketones **5** studied by Agami et al.[31] give lower ee's than the hydrindan/decalin system (42% ee with R = Me, Figure 3).[28c] In this case, the R substituent in **5** adopts an equatorial disposition and forces the α-hydrogen closer to a perfect axial arrangement, where it destabilizes the (*R*,*S*) transition structure by steric interaction with the carboxylate moiety.

(29) ω parameters are commonly used to describe out-of-plane deformations of enamines or amides; see ref 21.
(30) Cannizzaro, C. E.; Houk, K. N. *J. Am. Chem. Soc.* **2002**, *124*, 7163−7169.
(31) (a) Agami, C.; Sevestre, H. *J. Chem. Soc., Chem. Commun.* **1984**, *21*, 1385. (b) Agami, C.; Platzer, N.; Sevestre, H. *Bull. Soc. Chim. Fr.* **1987**, *2*, 358−360.

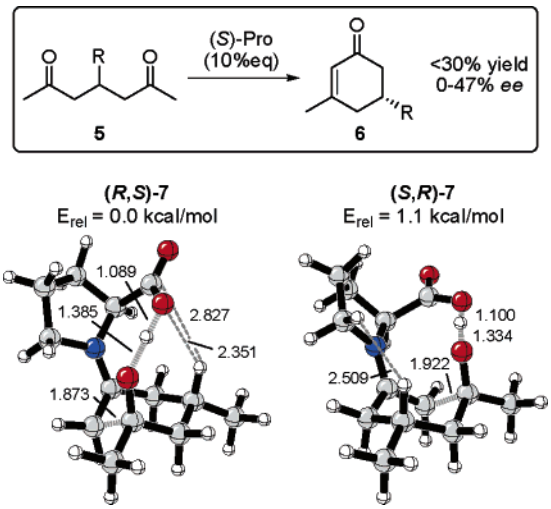

Figure 3. Transition states for the Agami aldol cyclizations.

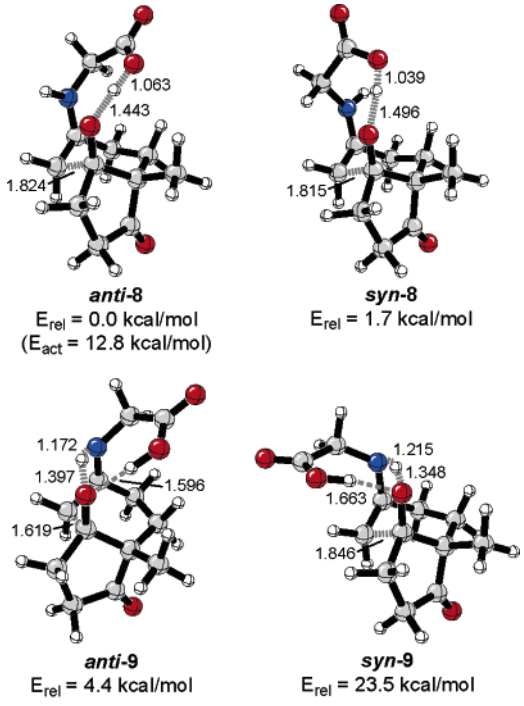

	anti-8	syn-8	anti-9	syn-9
ω_1 =	0°	10°	13°	-87°
ω_2 =	-5°	3°	27°	-50°
ω_3 =	158°	172°	163°	64°
ω_4 =	-163°	-159°	-124°	159°
ϕ =	-91°	120°	-95°	60°

Figure 4. Computed transition states for the glycine-catalyzed aldol cyclization of **1a**.

Primary Amino Acids. We have now explored the transition states of reactions involving other amino acids as catalysts. The study of acyclic primary amino acids starts with the simplest case, glycine. This amino acid is achiral, and no enantioselectivity is possible. However, this constitutes a good model to determine the preferred conformations of enamines derived from acyclic amino acids in general. Contrary to proline, anti and syn transition structures are possible for both *Si* and *Re* attacks with acyclic amino acids. Figure 4 shows the computed transition structures for the attack on the *Si* face of the carbonyl

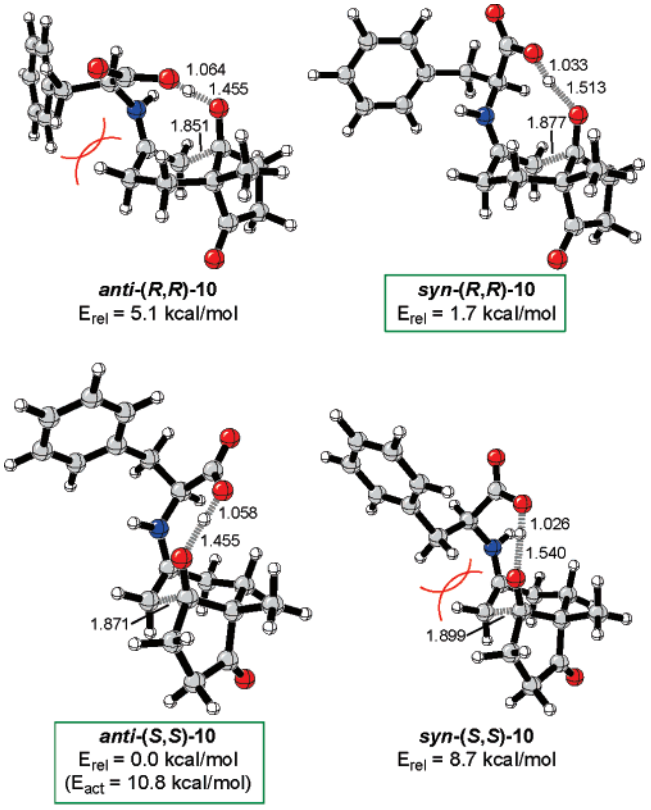

	anti-(*R*,*R*)	*syn*-(*R*,*R*)	*anti*-(*S*,*S*)	*syn*-(*S*,*S*)
ω_1 =	1°	-13°	2°	9°
ω_2 =	7°	7°	-9°	2°
ω_3 =	-160°	-174°	162°	171°
ω_4 =	168°	168°	-168°	-161°
ϕ =	58°	-123°	-94°	116°

Figure 5. Transition states for the (*S*)-phenylalanine-catalyzed aldol cyclization of **1a**.

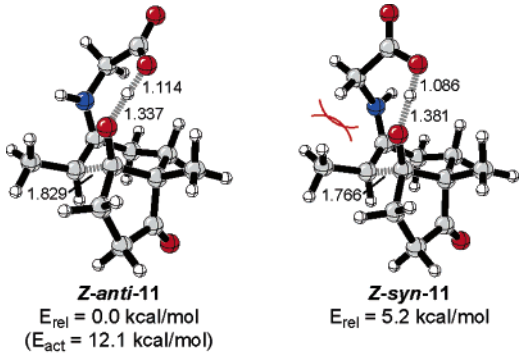

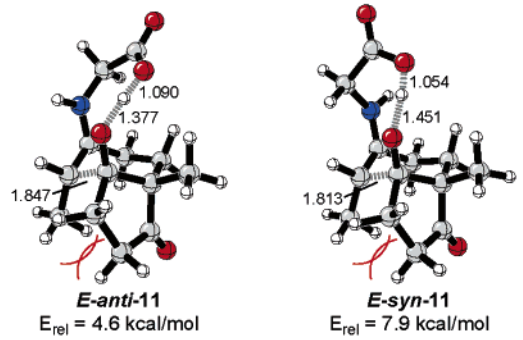

	Z-*anti*	*Z*-*syn*	*E*-*anti*	*E*-*syn*
ω_1 =	-5°	11°	-2°	9°
ω_2 =	-6°	14°	-5°	2°
ω_3 =	158°	175°	158°	171°
ω_4 =	-168°	-150°	-165°	-160°
ϕ =	-88°	108°	-91°	120°

Figure 6. Computed transition states for the glycine-catalyzed aldol cyclization of **1c**.

acceptor. The corresponding structures for attack on the *Re* face are enantiomers and, therefore, identical in energy.

The computed transition structures for the anti and syn modes of cyclization catalyzed by glycine (**8**) differ in energy by 1.7 kcal/mol, which is 1.6 kcal/mol lower than the corresponding difference in the (*S*)-proline-catalyzed reaction (**(***S*,*S*)- and **(***R*,*R*)-**4**). Primary amino acids allow a conformation of the carboxylic moiety that can give proton transfer with much lower distortion of the enamine system (small and similar values of ω_2 for both *anti*- and *syn*-**8**) than with proline (compare Figures 4 and 2). However, this conformation requires eclipsing of the C−H bond in the α-carbon with the incipient iminium N=C bond. The dihedral angle ϕ changes from its ideal value of ∼90° to ∼120°, which is an energetically less important distortion than the nonplanarity of the enamine, but still enough to provide a preference for the anti attack.

As with primary amine catalysis,[28b] primary amino acids could catalyze this reaction via the concerted N−H−O hydrogen transfer and C−C bond formation (**9**). These structures are nevertheless much higher in energy than those corresponding to the carboxylic acid catalysis (**8**), based upon the significant loss in enamine planarity. This is especially remarkable in TS *syn*-**9** (23.5 kcal/mol over TS *anti*-**8**), where the N−H bond is almost perpendicular to the C=C bond ($\omega_1 = -87°$).

The introduction of an amino acid substituent at the α-carbon makes the *Si* and *Re* attacks diastereomeric so that stereoselectivity is now possible. Figure 5 shows the B3LYP/6-31G(d) transition structures analogous to **8** but for the reaction catalyzed by (*S*)-phenylalanine. Only the structures with the preferred conformation of the benzyl group — a $C_{Ph}-C_{Ph}-C_\alpha-C_\beta$ dihedral ∼90°, and the best of the staggered arrangements with respect to $C_\alpha-C_\beta$ — are shown in each case. The energy barrier of the C−C bond-forming step, 10.8 kcal/mol, is similar to that of the corresponding proline-catalyzed process, 10.5 kcal/mol. With (*S*)-amino acids, the attack on the *Si* face to form the (*S*,*S*)-enantiomer is preferably anti (*anti*-(*S*,*S*)-**10**). This is due to the steric interaction between the methylene of the benzyl substituent and the enamine terminus in the syn attack (*syn*-(*S*,*S*)-**10**). This also explains why the syn transition state is preferred over the anti one for *Re* face attack (*syn*-(*R*,*R*)-**10**).

As in the glycine model (**8**), the energy difference between the most favorable (*S*,*S*)- and (*R*,*R*)-pathways is 1.7 kcal/mol. As discussed earlier, this is related to the necessity of the carboxyl to adjust the dihedral ϕ to an unfavorable arrangement (Figure 5). The 1.7 kcal/mol preference is about one-half that for the (*S*)-proline case, which accounts for the significant drop in enantioselectivity with (*S*)-phenylalanine. Our quantum mechanical studies, therefore, point toward the conformational flexibility of primary amino acids as the cause of their lower levels of asymmetric induction.

Stereoselectivity in the Cyclizations of Substituted Methyl Ketones

Figure 6 show the transition structures (**11**) for the glycine-catalyzed formation of ketols **2c**, the reaction of an ethyl ketone

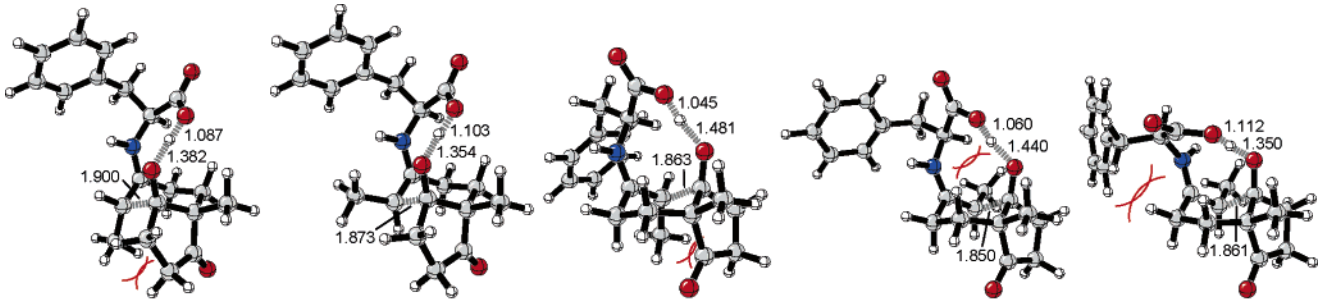

	anti-(S,S,S)	anti-(S,S,R)	syn-(R,R,R)	syn-(R,R,S)	anti-(R,R,S)
ω_1 =	1°	-2°	-9°	-13°	5°
ω_2 =	-9°	-9°	1°	-4°	9°
ω_3 =	162°	161°	-171°	-177°	-159°
ω_4 =	-170°	-172°	163°	160°	173°
ϕ =	-94°	-93°	-125°	-113°	56°

Figure 7. Transition states for the (*S*)-phenylalanine-catalyzed aldol cyclization of **1c**.

(R^1 = Me). All of these are rather similar to their nonsubstituted (R^1 = H) counterparts, **8**. Cyclization pathways involving the *E*-enamine are much less favored than those involving their *Z* counterparts, due to the steric hindrance between the methyl group and the cyclopentandione moiety in the *E*-isomer. The fact that the *Z*-enamine is more reactive also explains the significant increase in the energy difference between the anti and syn TSs (1.7 kcal/mol in the unsubstituted case, **8**, vs 5.2 kcal/mol in the substituted one, **11**). Most of this increase arises from the differential steric repulsion of the N substituents, H (*Z*-*anti*-**11**) vs CH (*Z*-*syn*-**11**). This is also reflected in the geometries: *Z*-*anti*-**11** presents values for ω and ϕ dihedral angles almost identical to those for *anti*-**8**, while in *Z*-*syn*-**11**, ω_2, ω_4, and ϕ are ~10° different than those in *syn*-**8** in order to minimize steric repulsion.

The transition structures for the glycine-catalyzed reaction, **11**, again provide a good model for chiral acyclic amino acids like (*S*)-phenylalanine (**12**); the transition states from the latter show geometries and energetics very similar to the ones derived from the former. Figure 7 also shows only the structures with the preferred conformation of the benzyl group in each case. For the same reason as noted in the glycine case, the *Z*-enamine from (*S*)-phenylalanine is more reactive than the *E*-isomer; calculations predict an almost complete diastereoselectivity for the all-cis isomer, (*S*,*S*,*R*)-**12**. This result cannot be compared directly with experiments because of the acidic reaction conditions used with these catalysts, leading directly to the enediones **3**. The energy difference between enantiomers (*S*,*S*,*R*)- and (*R*,*R*,*S*)-**12** increases substantially compared with that of the corresponding (*S*,*S*)- and (*R*,*R*)-**10** (5.6 vs 1.7 kcal/mol), in good agreement with the remarkable asymmetric induction of primary amino acids on the cyclization of triketones **1** ($R^1 \neq$ H). This is explained on the same basis as the anti−syn energy difference in the glycine model (**11**), i.e., the differential steric repulsion of the N substituents, H (*anti*-(*S*,*S*,*R*)-**12**) vs CH (*syn*-(*R*,*R*,*S*)-**12**). Figure 8 compares the bond angles around the partial C═N double bond in transition states catalyzed by (*S*)-phenylalanine. For the anti mode of addition, the geometries are almost identical in **10** (R^1 = H) and **12** (R^1 = Me), the bond angles being different by less than 0.4°. However, the steric repulsion

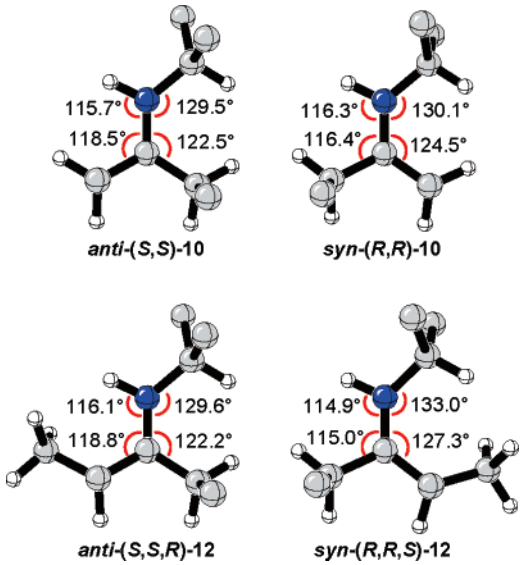

Figure 8. Effect of enamine substitution on the anti and syn geometries of (*S*)-phenylalanine-catalyzed aldol transition states. For clarity, only the atoms attached to the enamine system are shown.

of the enamine substituent ($R^1 \neq$ H) with the amino acid α-carbon in the syn transition states causes a distortion in the geometries. The two bond angles on the R^1 side in *syn*-(*R*,*R*,*S*)-**12** open by almost 3°, while the two on the other side close by 1.4° compared with the same angles in *syn*-(*R*,*R*)-**10** (Figure 8). Due to this interaction, syn and anti attacks of the *Z*-enamine on the *Re* face, *syn*- and *anti*-(*R*,*R*,*S*)-**12**, become comparable in energy. This contrasts with the unsubstituted case which lacks this interaction: the corresponding *syn*-(*R*,*R*)-**10** is 3.4 kcal/mol lower in energy than *anti*-(*R*,*R*)-**10**.

The methylene substituent on the proline nitrogen atom generates a considerable steric repulsion with the *Z*-enamine R^1 group. This leads to an inversion in the diastereoselectivity (Figure 9) as compared with that of the primary amino acid-catalyzed reaction (Figure 7). In agreement with experiments,[9] the most favored transition state for this reaction is (*S*,*S*,*S*)-**13**. For the (*S*)-proline-catalyzed cyclization of triketones **1**, the enantiomeric excesses for (*S*,*S*,*S*)-**2c** (R^1 = Me) and (*S*,*S*)-**2a** (R^1 = H) are predicted to be similar, since the *E*-enamine R^1

Table 2. Relative Energies (kcal/mol) of the Transition States at Different Levels of Theory for the Cyclization of **1a** Catalyzed by Proline, Glycine, or Phenylalanine

	(*S*)-Pro		Gly				(*S*)-Phe	
	(*S*,*S*)-**4**	(*R*,*R*)-**4**	*anti*-**8**	*syn*-**8**	*anti*-**9**	*syn*-**9**	*anti*-(*S*,*S*)-**10**	*syn*-(*R*,*R*)-**10**
B3LYP/6-31G(d)	0.0	3.3	0.0	1.7	4.4	23.5	0.0	1.7
B3LYP/6-31+G(d,p)//B3LYP/6-31G(d)	0.0	2.4	0.0	1.5	6.0	25.1	0.0	1.6
B3LYP/6-31+G(d,p)	0.0	2.5	0.0	1.4	6.0	25.1		

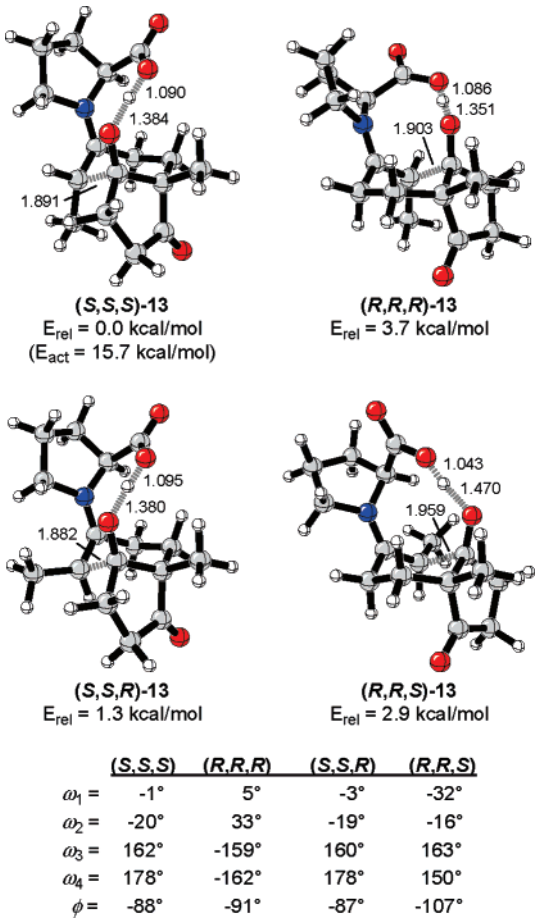

Figure 9. Transition states for the (*S*)-proline-catalyzed aldol cyclization of **1c**.

substituent is located on the opposite face of the chair-TS where chirality is being induced. Despite that, the presence of this group in this crowded area, facing the cyclopentanedione ring, is responsible for the substantial increase (5.2 kcal/mol) in the activation energy of this C−C bond-forming process as compared with that observed for (*S*,*S*)-**4**. This fact explains the difficulty of the proline-catalyzed cyclizations of **1** ($R^1 \neq H$) under neutral conditions.

Effects of Diffuse Functions

It has been argued that inclusion of diffuse functions in the basis set is required to accurately calculate hydrogen-bonding geometries and energies.[32] As shown in the present article, the transition states of aldol cyclizations catalyzed by amino acids feature a proton transfer in concert with the C−C bond formation. To test the effect of diffuse functions, all of the structures in Figures 2 and 4 (proline- and glycine-catalyzed transitions states for the cyclization of **1a**) have been fully optimized at the B3LYP/6-31+G(d,p) level. The optimized geometries obtained with this basis set present only slight changes from the ones obtained with B3LYP/6-31G(d). With the larger basis set, the distances between heavy atoms involved in the proton transfer are shortened by less than 0.024 Å for the O···O distance in structures **4** and **8** (Figures 2 and 4), and by less than 0.006 Å for the N···O distance in structures **9** (Figure 4). On the basis of the forming C−C bond distance, the transition states appear consistently earlier with the larger basis set, for **4** and **8** by 0.07−0.09 Å, and for **9** by less than 0.03 Å. The differences in the dihedral angles ω_{1-4} and ϕ between the two basis sets are lower than 3° for TSs **4** (Figure 2), and lower than 6° for TSs **8** and **9** (Figure 4). Since the geometry changes between the optimized structures with the two basis sets are subtle, the relative energies for the structures in Figures 2 and 4 from B3LYP/6-31+G(d,p)//B3LYP/6-31G(d) are almost identical to the ones from the full optimization with the larger basis set (Table 2). For the reaction catalyzed by phenylalanine (Figure 5), we have computed the energies of the two stereochemically relevant TSs, *anti*-(*S*,*S*)-**10** and *syn*-(*R*,*R*)-**10**, at this latter level (Table 2). Notice that, even though in all cases the syn−anti TS energy gap narrows with a larger basis set, this effect does not alter the conclusions about the origins of stereoselectivity in these reactions, nor the fact that the syn−anti TS energy difference is overestimated. As shown earlier in this article, the origin of the enantioselectivity arises from the distortion of the enamine planarity in the TS geometries. The portion of the geometry where the proton is being transferred is very similar in all of the TSs. These arguments can explain the little effect of diffuse functions on the computed energy differences (Table 2) in the aldol TSs as compared with the effect on hydrogen-bonding complexes.

Table 3. Comparison between the B3LYP/6-31G(d) Relative Energies (kcal/mol) of the Transition States Leading to Enantiomeric Products and the Highest Enantiomeric Excesses (%) Reported for Intramolecular Aldol Cyclizations of **1** Catalyzed by Proline and Phenylalanine

	$R^1 = H$		$R^1 \neq H$	
	DFT TS energy difference	exptl ee	DFT TS energy difference	exptl ee
Pro	3.3	96	3.7	93
Phe	1.7	25	5.4	95

Conclusions

Theoretical calculations at the B3LYP/6-31G(d) level satisfactorily reproduce the observed enantioselectivities in the amino acid-catalyzed intramolecular aldol cyclizations of triketones **1** (Table 3). The conformational flexibility of the primary amino acids allows a good alignment for the O−H···O hydrogen-bonding in the transition structures in either anti or syn approaches, which explains the lower enantioselectivity when

(32) Del Bene, J. E.; Person, W. B.; Szczepaniak, K. *J. Phys. Chem.* **1995**, *99*, 10705−10707.

they are used, instead of proline, as catalysts in the cyclization of **1** ($R^1 = H$). The high enantioselectivity found with primary amino acids in the substituted cases (**1** with $R^1 \neq H$) arises from the differential steric repulsion between the substituents on the enamine nitrogen, hydrogen (in anti-*Si*) and methylene (in syn-*Re*), with R^1 substituent of the *Z* enamine. These transition structures are lower in energy than their *E* counterparts because, in the latter, the enamine substituent is located in a more crowded area, so the all-cis bicyclic products are predicted to be the only diastereomers.

In the (*S*)-proline-catalyzed reaction, the steric repulsion with the R^1 substituent significantly destabilizes the *Z*-enamine, so the diastereomeric outcome is expected to be opposite to that observed with primary amino acids. This destabilization is responsible for the significant increase in the activation barrier for the C−C bond-forming step compared to the unsubstituted case.

Acknowledgment. We are grateful to the National Institute of General Medical Sciences, National Institutes of Health, for financial support of this research, and the National Computational Science Alliance, the National Science Foundation, and UCLA Academic Technology Services for computer resources. F.R.C. thanks Fundación Ramón Areces (Spain) for a postdoctoral fellowship.

Supporting Information Available: Cartesian coordinates of all of the structures with their computed total energies, and the full citation of Gaussian 98 (ref 26). This material is available free of charge via the Internet at http://pubs.acs.org.

JA0507620